SIAM J. APPL. MATH.
Vol. 64, No. 6, pp. 1839–1863

ANALYSIS OF STRESS-DRIVEN GRAIN BOUNDARY DIFFUSION. PART I*

JON WILKENING†, LEN BORUCKI‡, AND J. A. SETHIAN§

Abstract. The stress-driven grain boundary diffusion problem is a continuum model of mass transport phenomena in microelectronic circuits due to high current densities (electromigration) and gradients in normal stress along grain boundaries. The model involves coupling many different equations and phenomena, and difficulties such as nonlocality, complex geometry, and singularities in the stress tensor have left open such mathematical questions as existence of solutions and compatibility of boundary conditions. In this paper and its companion, we address these issues and establish a firm mathematical foundation for this problem.

We use techniques from semigroup theory to prove that the problem is well posed and that the stress field relaxes to a steady state distribution which, in the nondegenerate case, balances the electromigration force along grain boundaries. Our analysis shows that while the role of electromigration is important, it is the interplay among grain growth, stress generation, and mass transport that is responsible for the diffusive nature of the problem. Electromigration acts as a passive driving force that determines the steady state stress distribution, but it is not responsible for the dynamics that drive the system to steady state.

We also show that stress singularities may develop near grain boundary junctions; however, stress components directly involved in the diffusion process remain finite for all time. Thus, we have identified a mechanism by which large "hidden" stresses may develop that are not directly involved in the diffusion process but may play a role in void nucleation and stress-induced damage.

Key words. grain boundary, diffusion, electromigration, elasticity, semigroups

AMS subject classifications. 35Q72, 47D03, 74F99

DOI. 10.1137/S0036139903438235

1. Introduction.

A microelectronic circuit consists of a silicon substrate with doped regions that function as circuit elements (transistors, diodes, resistors, and capacitors), metal lines and vias (interconnects) that connect the circuit elements together, intermetallic dielectric material that keeps the interconnects in place and insulated from each other, various oxide layers and diffusion barriers that are primarily needed in the manufacturing stage to control the doping process and keep the metal from diffusing into the silicon, and passivation to keep all the components in place and protected [28, 33].

A typical interconnect line might be an alloy of Al-0.5%Cu, have dimensions of $0.5 \times 0.5 \times 300$ microns, and carry a current density of 20 $m\text{A}/\mu m^2$. As electrons

*Received by the editors December 6, 2002; accepted for publication (in revised form) November 26, 2003; published electronically August 4, 2004.
http://www.siam.org/journals/siap/64-6/43823.html

†Courant Institute of Mathematical Sciences, New York, NY 10012 (wilken@cims.nyu.edu). The research of this author was supported in part by a Department of Energy Computational Science Graduate Student Fellowship while the author was at U.C. Berkeley; by the Applied Mathematical Sciences subprogram of the Office of Energy Research, U.S. Department of Energy, under contract DE-AC03-76SF00098; and by the National Science Foundation through grant DMS-0101439.

‡Motorola, Inc., Tempe, AZ 85284 (Len.Borucki@intelligentplanar.com). The research of this author was supported in part by the Division of Mathematical Sciences of the National Science Foundation, University-Industry Program.

§Department of Mathematics and Lawrence Berkeley National Laboratory, University of California, Berkeley, CA 94721 (sethian@math.berkeley.edu). The research of this author was supported in part by the Applied Mathematical Sciences subprogram of the Office of Energy Research, U.S. Department of Energy, under contract DE-AC03-76SF00098 and by the Division of Mathematical Sciences of the National Science Foundation.

flow through the line, they are scattered by imperfections in the crystal lattice of the metal and impart momentum to the ion cores. This "electron wind" force is stronger than the opposing direct force of the electric field, so ions are transported in the same direction as the flow of electrons. This process is known as electromigration; it is a dominant failure mechanism in microelectronic devices.

Grain boundaries, void surfaces, and passivation interfaces are fast diffusion paths along which the diffusion constant typically is seven to eight orders of magnitude higher than in the grains; therefore, most of the mass transport occurs at these locations. The inhomogeneous redistribution of atoms leads to the development of stresses in the line. Stress gradients along grain boundaries and surface tension at void surfaces both contribute to the flux of atoms, usually opposing the electromigration term and increasing the lifetime of the line. Significant residual stresses left over from thermal contraction during the manufacturing process also affect the formation of voids and the transport of atoms.

As microelectronic circuits become smaller and current densities become higher, failure due to electromigration damage becomes an ever increasing problem in the design of circuits. Many theoretical models have been proposed to explain the role of various combinations of electromigration, stress gradients, diffusion, temperature, anisotropy, surface tension, and hillock formation on the mass transport of atoms in the bulk grains, along void surfaces, along grain boundaries, and at passivation interfaces. A useful reference written from the engineering perspective is the review article by Ho and Kwok [14]; see also [27]. The concept of the electron wind force was formulated by Fiks [9] and by Huntington and Grone [15]. In his experimental work in the 1970s, Blech [2] studied the behavior of thin films of aluminum and titanium-nickel when large currents were passed through them and demonstrated the existence of a threshold current density below which no damage occurs, which varies inversely with the stripe length. Shortly thereafter, Blech and Herring [3] offered the explanation that stress gradients were developing along grain boundaries in the sample to counter the electron wind force, but they could be sustained only up to a critical threshold. Once this threshold was reached, there was no physical mechanism to stop the transport of material, and the stripe eroded at one end and formed hillocks at the other.

Recent models of these phenomena were described by Mullins [21], Cocks and Gill [6], Korhonen et al. [18], Sarychev et al. [25], and Kirchheim [17]. The Mullins paper presents a nice overview of mass transport along surfaces and grain boundaries and discusses cobble creep and grain boundary grooving. The paper by Cocks and Gill gives a variational approach to the dynamics of grain boundary motion associated with decreasing grain boundary area; they did not include stress in their model. The papers [25] and [17] deal primarily with electromigration, stress-driven diffusion, and vacancy generation in the grains, while [18] focuses on electromigration and grain boundary diffusion. The latter three papers use a statistical argument about the orientation of the grain boundaries in order to model the stress as a scalar variable instead of a tensor; one should keep in mind, however, that for any particular sample, the grain boundaries have a specific geometry, and singularities can occur in the stress field that are ignored with this simplifying assumption.

Bower, Craft, Fridline, and collaborators use an advancing front algorithm to generate a sequence of adaptive, evolving finite element meshes to study grain growth, void evolution, hillock formation, and grain boundary sliding for possibly anisotropic materials responding to stress, surface tension, thermal expansion, and electromi-

gration; see, e.g., [4, 10]. They use interesting semi-implicit techniques to overcome timestep limitations due to the stiffness of the equations, and they use Lagrange multipliers to determine the normal stress along grain boundaries.

An alternative approach based on the theory described in this paper is presented in [30, 26], where a new singularity capturing the least squares finite element method is developed to study the effect of singularities in the stress field on the grain boundary diffusion process. Further references to the literature on numerical methods for grain growth and void evolution may be found there.

Mathematical analysis of the partial differential equations involved is largely absent in the electromigration literature. There are several reasons for this. First, there is no universal agreement in the electromigration community on exactly how all the phenomena fit together, especially at junctions where grain boundaries meet voids or other grain boundaries, and the process of void nucleation is far from understood. Second, the problem is very complicated, with many different (stiff) phenomena coupled together in a nonlocal, nonlinear way. Growth rates depend on taking derivatives of stress components along grain boundaries and curvatures along surfaces. Boundary conditions specify the gradient of the normal stress at junctions where the stress field is singular. Many of the equations couple the displacement field to the stress field, and it is difficult to visualize how this constrains the evolution of the system. Both displacement and flux boundary conditions are specified at junctions where grain boundaries meet the outer walls; in simpler problems such as the heat equation, this would overspecify the boundary conditions. As a result of these and similar difficulties, one typically has a long list of equations reflecting various principles such as mass conservation and chemical potential continuity that one would like to use as a model. But occasionally, incomplete physical reasoning can lead to mathematically ill-posed problems; therefore, it is important to develop a rigorous justification for the collection of equations to ensure a self-consistent model.

The goal of this paper is to provide a mathematical framework in which we can analyze a modest subset of the phenomena mentioned above. We assume there are no voids in the structure, and we work within the framework of linear elasticity (small strain and small grain growth). This may be thought of as the linearization of a nonlinear grain boundary migration theory. Most of the difficult problems mentioned above persist in this setting. The equations are nonlocal and couple together many different stiff phenomena that relate rates of change of displacement jumps to spatial derivatives of the normal stress. The boundary conditions specify the gradient of the normal stress at locations where the stress tensor becomes singular. And the geometry of the problem involves the complicated branching structure of a grain boundary network which does not have a natural ordering or orientation of its segments. The same approach is taken in [30].

In section 2, we exhibit the equations in dimensionless form and briefly describe the physical considerations that lead to these equations. Our main contribution here is to model the net grain growth along the grain boundary Γ as the jump in a normal component of the displacement across Γ, thinking of it as a scalar function g defined on Γ. This is identical to what Bower and Craft did in [4], except that they viewed each side of the grain boundary as a moving interface (in parallel with their treatment of void surfaces) and did not single out g as important. They derived an equation for the change Δg (denoted Δu_n in their paper) in a timestep but used it only to update the displacements $\mathbf{u}$ on each side of the grain boundary. The advantage of treating g as a time evolving *function* defined on the grain boundary (which is

fixed in the reference configuration) is that we are able to recast the problem as an ordinary differential equation on a Hilbert space and to apply techniques of semigroup theory to prove the equations are well posed. The difficulties due to nonlocality, the existence of singularities, and the complicated nature of the boundary conditions are all absorbed into two unbounded operators L and S, which turn out to possess many nice properties, such as self-adjointness, discrete spectra, and positivity (or negativity). An overview of this procedure is given in section 3, and full details are presented in section 6.

In section 4, we define the grain boundary normal stress problem and the operator S, which is a type of Dirichlet-to-Neumann map that maps the displacement jump g across Γ to the normal stress $\eta = \mathbf{n} \cdot \sigma \mathbf{n}$ on Γ. We state the important properties of S (which are proved in the companion paper [31]) and identify a new class of grain boundaries, which we call *degenerate*. Throughout this paper, we assume the grain boundary network is nondegenerate in order to simplify the presentation. The degenerate case is dealt with in [31].

In section 5, we analyze the operator L $(= -\frac{\partial^2}{\partial s^2})$ on the grain boundary network. The most important properties of this operator are that it is positive and self-adjoint, its domain $\mathcal{D}(L)$ consists only of functions that satisfy continuity and flux boundary conditions (useful for proving that the normal stress η has these properties), and the domain of $L^{\frac{1}{2}}$ is precisely $H^1(\Gamma)$ (useful in specifying the Hilbert space in which η evolves). The boundary conditions of chemical potential continuity and flux balance at junctions turn out to be exactly what are needed for these results to hold.

In section 6, we show that the equation governing the evolution of normal stress (namely, $\eta_t = SL\eta$) generates an analytic semigroup $\{E_t : t \geq 0\}$ of bounded linear operators on $H^1(\Gamma)$. The primary difficulties that arise have to do with the fact that L (and in the degenerate case, S) has a nontrivial finite dimensional kernel which must be dealt with using projections. We also discuss the role of electromigration as a passive driving force, the enforcement of boundary conditions, and the development of stress singularities near corners and grain boundary junctions.

Finally, in the Appendix, we study an infinite interconnect line with a single grain boundary running through its center, which provides insight into the nature of the diffusion process without the complication of boundary conditions and singularities.

2. Problem statement. In this section, we describe a two dimensional continuum model of electromigration and stress-driven grain boundary diffusion in the linear regime of small strain, small grain growth elasticity. The reference configuration (including the location of the grain boundary in the reference configuration) remains fixed, while the stress and displacement fields defined on this domain evolve in time.

A grain is a region where the atoms are aligned in a regular lattice. A grain boundary is an interface between two grains where the lattice structure becomes disorganized as the lattice alignment changes from one side to the other. In our (continuum) model, we ignore details of lattice alignment and assume all grain boundaries have equivalent properties.

The grain boundaries are assumed to be fast diffusion paths along which atoms are transported much more easily than in the bulk grains. At each point on the grain boundary, we have a flux J of atoms traveling along the grain boundary. J has units of surface flux ($\mathrm{cm}^{-1}\mathrm{s}^{-1}$), where we consider our two dimensional domain to have a thickness δ in the third dimension. If a portion of the grain boundary has more atoms flowing into it than out, the atoms incorporate themselves into the lattice of the adjacent grains and cause the grains to move apart to make room for the new

atoms. At the same time there will be a net flux of atoms out of other regions of the grain boundary, where atoms are removed from the lattice of each grain and the grains move together so as not to leave a gap.

Although our analysis of this problem does not rely on the grain boundaries being straight, we have omitted curvature-driven grain boundary motion from our model. For this reason, we assume that the grain boundaries are initially straight and that as grain growth occurs, the appropriate fraction of atoms attaches to each side of the grain boundary so that Γ remains fixed in the spatial (stressed) configuration. We adopt an Eulerian viewpoint where the reference configuration on which the stress and displacement fields are defined is the spatial configuration, and the natural (unstressed) shape of each grain changes in time as material is added to (or removed from) its boundary. For a given deformation φ mapping the natural state to the stressed state, the displacement is defined as $\mathbf{u}(x) = x - \varphi^{-1}(x)$ instead of $\varphi(x) - x$. The linearized equations of elasticity [20, 5] are the same in the material and Eulerian viewpoints.

We assume the interconnect line consists of several disjoint bounded polygonal grains Ω_k, and we denote their union (an open set) by $\Omega = \bigcup_k \Omega_k$. $\overline{\Omega}$ is assumed to be connected; see Figure 2.1. We denote the outer boundary (the "walls") of the domain by $\Gamma_0 = \partial(\overline{\Omega})$ and the grain boundary network by $\Gamma = (\partial\Omega \setminus \Gamma_0)^-$. Γ consists of N closed line segments $\Gamma = \bigcup_{j=1}^{N} \Gamma_j$. Each segment is given an arbitrary orientation (a unit tangent vector $\mathbf{t}_j$) and an arclength parameter s which increases in the $\mathbf{t}_j$ direction. The unit normal $\mathbf{n}_j$ points from right to left facing along $\mathbf{t}_j$. We do not impose the Young condition, requiring that grain boundaries meet at 120° angles, since it is not required for well posedness unless curvature is included as a driving force.

The net grain growth g is defined on Γ as the jump in normal component of displacement across the grain boundary:

$$g(x) := [\mathbf{u}(x^+) - \mathbf{u}(x^-)] \cdot \mathbf{n}_j \qquad (x \in \Gamma_j). \tag{2.1}$$

It represents the distance the original grains have separated to accommodate the new material that occupies that space; see Figure 2.2. In the Eulerian picture, $g(x) = [\varphi^{-1}(x^-) - \varphi^{-1}(x^+)] \cdot \mathbf{n}$ is the amount that opposite sides of the grain boundary at x would overlap if the grains were allowed to pass through each other to achieve their stress-free shapes. This overlap corresponds to new material added during the diffusion process.

In Figure 2.3, we list the equations and boundary conditions in nondimensional form. We choose an arbitrary length scale L ($\sim 1\mu$m) and define the timescale $t_0 = \frac{kTL^3}{\nu_b D_b \Omega_a^2 \mu}$, where k is the Boltzmann constant, T is temperature, D_b is the diffusion constant for grain boundary surface diffusion at temperature T, ν_b is the number of participating atoms per unit area, Ω_a is the volume of an atom in the atomic lattice, and μ is the shear modulus. See [21] for typical values of these parameters. We then define the dimensionless variables

$$\tilde{x} = \frac{x}{L}, \quad \tilde{t} = \frac{t}{t_0}, \quad \tilde{\mathbf{u}} = \frac{\mathbf{u}}{L}, \quad \tilde{\sigma} = \frac{\sigma}{\mu}, \quad \tilde{\psi} = \frac{|Z^*|e}{\Omega_a \mu}\psi, \quad \tilde{J} = \frac{\Omega_a t_0}{L^2} J, \quad \text{etc.}, \tag{2.2}$$

and rewrite the equations (see [4, 30]) in terms of these variables (dropping the tildes). Z^*e is a phenomenological effective charge for an ion in the lattice; $e = |e|$ is the elementary electric charge; and for a good conductor [21, 29], $Z^* \approx -5$. This means the electron wind force is stronger than the opposing direct force of the electric field.

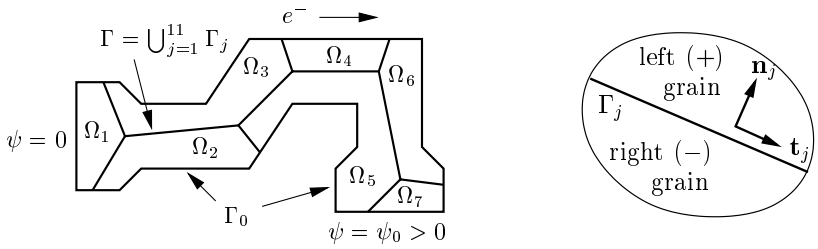

FIG. 2.1. *Left: geometry of an interconnect line. Right: arbitrarily assigned orientation of grain boundary segment determines tangential and normal directions, left and right grain labels, etc. The normal vector* $\mathbf{n}_j$ *points from right to left when facing along the* $\mathbf{t}_j$ *direction.*

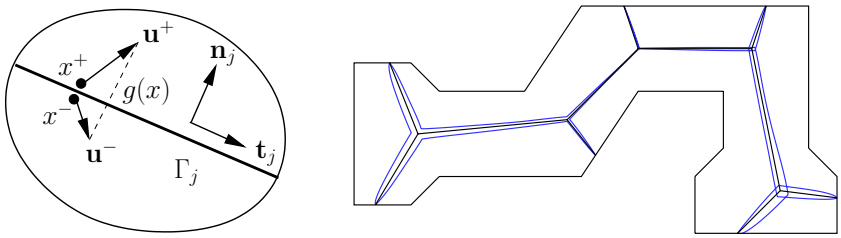

FIG. 2.2. *Left:* $g(x)$ *is the jump in normal component of displacement across* Γ *at* x*. The sign of* g *is independent of the orientation chosen for the segment. Right: exaggerated view of the natural state of each grain obtained by plotting* $x - C\mathbf{u}(x^{\pm})$*,* $x \in \Gamma$*, with a suitable* $C > 0$*. Grains must be zipped together (*$g < 0$*) on the left and pushed apart (*$g > 0$*) on the right in order to fit together.*

Electric Potential

1. $\nabla^2 \psi = 0$
2. $\partial_n \psi = 0$
3. $\psi = 0$
4. $\psi = \psi_0$
5. Grain boundaries are invisible to ψ

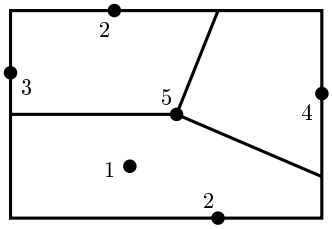

Elasticity and Grain Growth

1a. $\mu \Delta \mathbf{u} + (\lambda + \mu) \nabla (\nabla \cdot \mathbf{u}) = 0$
2a. $\mathbf{u} = 0$
3a. $\mathbf{u}(x^+) - \mathbf{u}(x^-) = g(x)\mathbf{n}$
3b. $\sigma(x^+) = \sigma(x^-)$
3c. $\mathbf{n} \cdot \sigma(x)\mathbf{n} = \eta(x)$
3d. $\partial_t g = -\partial_s^2(\eta + \psi)$ $\begin{cases} J = \partial_s(\eta + \psi) \\ g_t + J_s = 0 \end{cases}$
4a. $g = 0$
4b. $\partial_s(\eta + \psi) = 0$
5a. $g(x_1)\mathbf{n}_1 + g(x_2)\mathbf{n}_2 + g(x_3)\mathbf{n}_3 = 0$
5b. $\eta(x_1) = \eta(x_2) = \eta(x_3)$
5c. $\partial_{s_1}(\eta + \psi) + \partial_{s_2}(\eta + \psi) + \partial_{s_3}(\eta + \psi) = 0$

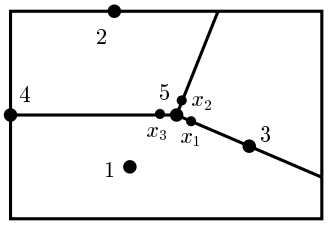

Initial Condition: $g \equiv 0$

FIG. 2.3. *Summary of equations and boundary conditions. Segments are assumed (in this figure only) to be parameterized away from the triple junction to avoid minus signs.*

The electric potential ψ is found by solving the Laplace equation under the assumption that the grain boundaries do not significantly affect the flow of current in the line. The displacement field $\mathbf{u}$ is found by solving the Lamé equations of linearized elasticity (assuming plane strain). The stress tensor satisfies Hooke's law,

$$\sigma = 2\mu\epsilon + \lambda \operatorname{tr}(\epsilon) I, \tag{2.3}$$

where λ and μ are the Lamé coefficients, $\epsilon_{ij} = \frac{1}{2}(\partial_i u_j + \partial_j u_i)$ are the components of the strain tensor, and $\operatorname{tr}(\cdot)$ is the trace operator; see [20, 5].

Referring to Figure 2.3, 2a enforces the requirement that the displacement is zero at the outer walls (passivation). In 3a, we assume that the grains do not slide tangentially relative to each other, and we define the displacement jump g. In 3b, we enforce the local balance of forces (tractions) across the grain boundary, which together with the no-sliding assumption implies that all components of the stress tensor are continuous across grain boundaries. In 3c, we define the normal stress η on the grain boundary, which is well defined by 3b.

Equation 3d in Figure 2.3 is the main evolution equation, which gives the grain growth rate in terms of the normal stress and the electrostatic potential. This equation is a consequence of the continuity equation, the Einstein–Nernst equation, the Blech–Herring model of the chemical potential of an atom in a grain boundary of a stressed solid [3, 30], and electromigration:

$$\partial_t g + \Omega_a \partial_s J = 0 \qquad \text{(continuity equation)}, \tag{2.4}$$

$$J = -\tfrac{\nu_b D_b}{kT} \partial_s \mu_b \qquad \text{(Einstein–Nernst, } \mu_b = \text{chemical potential)}, \tag{2.5}$$

$$\mu_b = \mu_0 - \Omega_a \sigma_{nn} \qquad \text{(Blech–Herring, } \mu_0 = \text{const)}, \tag{2.6}$$

$$\partial_s \mu_b \to \partial_s \mu_b + Z^* e\, \partial_s \psi \qquad \text{(electron wind force, } Z^* e < 0), \tag{2.7}$$

$$J = \tfrac{\nu_b D_b}{kT} (\Omega_a \partial_s \sigma_{nn} + |Z^* e|\, \partial_s \psi) \quad \text{(flux before nondimensionalizing)}. \tag{2.8}$$

Note that qualitatively, atoms are transported from regions of compression to regions of tension and travel against the electric field $\mathbf{E} = -\nabla\psi$ in the same direction that electrons flow. Here, $\partial_s \psi$ is the derivative of $\psi\big|_\Gamma$ with respect to arc length, so $-\partial_s \psi = \mathbf{E} \cdot \mathbf{t}$ is the component of the electric field along the grain boundary.

Equation 4a in Figure 2.3 follows from 2a and 3a but is worth recording as a boundary condition on g. Equation 4b enforces zero flux at gb-wall junctions: atoms are not allowed to flow in or out of the network where the grain boundary meets passivation, so global mass conservation should hold. Equation 5a is a compatibility requirement following from 3a: if we start in one grain and follow the jump in displacement around a triple junction, we have to end up with the original displacement when we return. (The point x_i here is infinitesimally close to the triple junction on segment i.) Finally, equations 5b and 5c enforce chemical potential continuity and flux balance at triple junctions, respectively.

3. Strategy. Thus far, each equation represents either a definition (of g or η) or some physical requirement such as chemical potential continuity or mass conservation. The next task is to find a way to organize them so that mathematical questions such as well posedness can be addressed. One major challenge is to identify the role played by singularities in the stress field near junctions and to understand the sense in which 4b, 5b, and 5c of Figure 2.3 can be expected to hold in light of these singularities. Another goal is to find a way to untangle the equations and boundary conditions in order to handle the nonlocal nature of expressions relating the displacement jump g

to the normal stress η; placing local constraints on one imposes (rather awkward) global constraints on the other via the Lamé equations. It is not immediately obvious that the evolution 3d is compatible with conditions 4a–5c.

Our approach is to recast the problem as an ordinary differential equation on a Hilbert space, writing the equation in terms of the normal stress η and absorbing all the boundary conditions into the operators. In this way we take advantage of linearity and gain insight into the role played by each of the boundary conditions in the well posedness of the problem.

3.1. A type of Dirichlet-to-Neumann map. Equations 1a–3c in Figure 2.3 can be thought of as providing a mapping between the jump in displacement g and the normal stress η. If we are given one (in some appropriate space), the other can be determined by solving the elasticity equations. There is a duality between g and η embodied in the energy relation

$$E = -\frac{1}{2}\int_\Gamma \eta g \, ds, \tag{3.1}$$

relating the elastic energy stored in the grains to the work done at the grain boundaries to accommodate the accumulation or depletion of atoms there. See the companion paper [31] for further details.

We denote the operator that maps a given grain growth function g on Γ to the corresponding normal stress η by

$$S : \mathcal{D}(S) \to L^2(\Gamma) : g \mapsto \eta \qquad \text{(grain growth to normal stress map)}. \tag{3.2}$$

Although S is unbounded, it turns out to be self-adjoint and negative (essentially due to (3.1)), and its domain is dense in $L^2(\Gamma)$. Moreover, S has a compact pseudoinverse B such that SB is the identity (nondegenerate case) or differs from the identity by a finite rank projection (degenerate case). These properties are discussed in section 4 and proved in [31].

3.2. The second derivative operator. We define the operator $L : \mathcal{D}(L) \to L^2(\Gamma)$ to be the negative of the second derivative operator with respect to arc length on each grain boundary segment. If η is twice continuously differentiable on each Γ_j and satisfies certain boundary conditions at the junctions, then $\eta \in \mathcal{D}(L)$ and the restriction of $L\eta$ to the interior of Γ_j is given by

$$L\eta(x) = -\frac{\partial^2 \eta}{\partial s^2} \qquad (x \in \Gamma_j^o). \tag{3.3}$$

In section 5 we will show that boundary conditions 4b, 5b, and 5c from Figure 2.3 enforcing mass conservation and chemical potential continuity are exactly what are needed for some of the most useful properties of L on the unit interval to carry over to the more complicated branching structure of a grain boundary network. In particular, L is self-adjoint, positive, and densely defined, and its kernel is finite dimensional. Moreover, if $L^{\frac{1}{2}}$ is modified by a finite rank projection to remove its kernel, it becomes an isomorphism from $H^1(\Gamma)$ onto $L^2(\Gamma)$, which is important in our proof of well posedness.

3.3. An ordinary differential equation on a Hilbert space. The evolution of the jump in displacement g is governed by equation 3d of Figure 2.3, namely,

$$g_t = -\partial_s^2(\eta + \psi) = L(Sg + \psi). \tag{3.4}$$

Applying S to (3.4), we obtain

$$\eta_t = SL(\eta + \psi). \tag{3.5}$$

The term ψ is acting as a passive driving force in (3.4) and (3.5). In general, if the equation

$$\frac{dx}{dt} = Ax, \qquad x(0) = x_0, \tag{3.6}$$

generates a strongly continuous semigroup $\{E_t : t \geq 0\}$ of bounded linear operators on a Banach space X [13, 32, 16, 1], then for $f \in X$ the solution to the equation

$$\dot{x} = A(x + f), \qquad x(0) = x_0, \tag{3.7}$$

is given by

$$x(t) = E_t(x_0 + f) - f \qquad (t \geq 0). \tag{3.8}$$

In section 6, we will show that the equation

$$\eta_t = SL\eta, \qquad \eta(x, t = 0) = \eta_0(x), \tag{3.9}$$

generates such a semigroup in $H^1(\Gamma)$, so the evolution of the normal stress η with initial condition η_0 (usually taken to be zero) is given by

$$\eta(t) = E_t(\eta_0 + \psi) - \psi. \tag{3.10}$$

In the nondegenerate case, the evolution of g may be obtained directly from that of η via $g(t) = B\eta(t)$, but in the degenerate case this is not so. In both cases, the normal stress η evolves to a steady state stress distribution, but in the degenerate case the displacement jump g can grow linearly without bound along certain growth modes which are not suppressed by the stress-driven diffusion mechanism. The picture is suggestive of continental drift in plate tectonics, but the underlying physical mechanism is entirely different; see [31].

4. The grain boundary normal stress problem. In this section we describe the interface boundary conditions that are imposed when solving the Lamé equations, introduce the notion of degeneracy of a grain boundary network, and define the operators S and B. Rigorous proofs of the key properties of S and B are presented in the companion paper [31].

DEFINITION 4.1 (grain boundary normal stress). *Given a function $\eta \in L^2(\Gamma)$, find the displacement field $\mathbf{u} \in H^1(\Omega)^2$ satisfying $\mu\Delta\mathbf{u} + (\lambda + \mu)\nabla(\nabla \cdot \mathbf{u}) = 0$ in the interior of each grain subject to the boundary conditions*

$$\mathbf{u}(x) = \mathbf{0} \qquad (x \in \Gamma_0), \tag{4.1}$$

$$[\mathbf{u}(x^+) - \mathbf{u}(x^-)] \cdot \mathbf{t}_j = 0 \qquad (x \in \Gamma_j), \tag{4.2}$$

$$[\sigma(x^+) - \sigma(x^-)]\mathbf{n}_j = \mathbf{0} \qquad (x \in \Gamma_j), \tag{4.3}$$

$$\mathbf{n}_j \cdot \sigma(x)\mathbf{n}_j = \eta(x) \qquad (x \in \Gamma_j). \tag{4.4}$$

Here $H^1(\Omega)$ denotes the set $\{w \in L^2(\Omega) : w|_{\Omega_k} \in H^1(\Omega_k)\}$, so the jump in normal component of displacement $[\mathbf{u}(x^+) - \mathbf{u}(x^-)] \cdot \mathbf{n}_j$ is permitted to be nonzero for $x \in \Gamma_j$.

To make sense of the boundary condition (4.4) for a general $\eta \in L^2(\Gamma)$, a suitable notion of weak solution must be defined. This is done in [31], where it is shown that for certain "degenerate" grain boundary networks, additional compatibility conditions must be satisfied by η for a solution $\mathbf{u}$ to exist, and when it does exist, it is not unique. This situation may be characterized as follows.

DEFINITION 4.2. *A grain boundary network is said to be* degenerate *if there exists a nonzero displacement field* $\mathbf{u}$ *consisting of infinitesimal rigid body motions*

$$u_1\big|_{\Omega_k} = a_k - c_k y, \quad u_2\big|_{\Omega_k} = b_k + c_k x \quad (a_k, b_k, c_k \text{ constants}) \tag{4.5}$$

such that the boundary conditions (4.1)–(4.4) *hold with* $\eta \equiv 0$. *The jump in normal component of displacement across grain boundaries is permitted to be nonzero.*

In other words, degeneracy occurs when stress-free infinitesimal rigid body motions exist (grain by grain) that are zero at the outer walls and satisfy a no-sliding condition across grain boundaries. An algorithm for finding the degeneracies of any grain boundary network is presented in [31], where it is shown that degeneracy is a consequence of pathologies such as junction angles greater than 180° or a large number of quadruple (or higher) order junctions. In this paper we explicitly assume the grain boundary network is nondegenerate, leaving the general case to [31]. This substantially simplifies our proof of well posedness while retaining the key ideas.

DEFINITION 4.3. *When the grain boundary network is nondegenerate, the normal stress to grain growth operator* $B : L^2(\Gamma) \to L^2(\Gamma) : \eta \mapsto g$ *is defined via*

$$(B\eta)(x) = [\mathbf{u}(x^+) - \mathbf{u}(x^-)] \cdot \mathbf{n}_j \qquad (x \in \Gamma_j), \tag{4.6}$$

where $\mathbf{u}$ *is the (unique) solution to the grain boundary normal stress problem corresponding to* η.

Remark 4.4. As discussed in Figure 2.2, this definition is independent of the orientation chosen for each segment Γ_j.

DEFINITION 4.5. *When the grain boundary network is nondegenerate, the operator* $S : \mathcal{D}(S) \to L^2(\Gamma) : g \mapsto \eta$ *is defined as the inverse of* B. *In other words,* $\mathcal{D}(S) := \text{range}(B)$ *and for* $y \in \mathcal{D}(S)$, Sy *is the unique* x *such that* $Bx = y$.

THEOREM 4.6. B *is self-adjoint, negative, and compact.* S *is self-adjoint, negative, closed, and densely defined. In the nondegenerate case considered here,* B *is also injective and has dense range.*

Proof. See [31] for the proof. ∎

Remark 4.7. The domain $\mathcal{D}(S)$ is quite complicated due to the variety of ways self-similar solutions of the Lamé equations can behave near grain boundary junctions; see [26, 30]. In particular, even for smooth functions η that are continuous at junctions, $g = B\eta$ generally will be discontinuous at junctions and exhibit infinite slopes. As a result, it would be very difficult to define S directly by setting up a boundary value problem specifying g along Γ such that the resulting normal stress η is always meaningful in the trace sense. By defining S as we have, we can derive its properties by studying the compact operator B, which is well defined for all $\eta \in L^2(\Gamma)$. Moreover, this approach allows us to explain how it is possible to impose boundary conditions involving the normal stress at junctions where the stress tensor develops singularities: the components directly involved in the diffusion process remain finite and well behaved for all time (and satisfy the boundary conditions) while other components of the stress tensor blow up; see section 6.4.

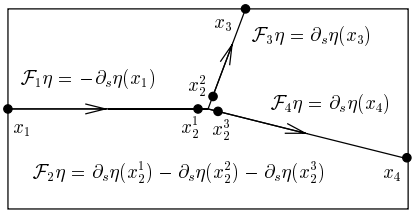

FIG. 5.1. *The flux $\mathcal{F}_i\eta$ into junction i is a sum over incident segments j of slopes $\pm\partial_s\eta$.*

5. The Poisson equation on the grain boundary network. In this section we show that the operator L is self-adjoint and positive, that there is a compact pseudoinverse G for L such that $I - LG$ is a finite rank projection onto $\ker(L)$ in $L^2(\Gamma)$, and that $A^{\frac{1}{2}} := (L + I - LG)^{\frac{1}{2}}$ is an isomorphism from $H^1(\Gamma)$ onto $L^2(\Gamma)$. We also characterize $\mathcal{D}(L)$ and $\mathcal{D}(L^{\frac{1}{2}})$ and identify the kernel of L as the set of functions that are constant on each connected component of Γ. Although these facts are well known in the case of the Neumann problem on the unit interval, several nonobvious tricks must be used to prove them for a network, and notation must be introduced that can cleanly handle the lack of a natural ordering and orientation for the grain boundary segments. In particular, we point out that not every function on a network with loops has a continuous antiderivative (unless its integral around each loop is zero).

5.1. Boundary conditions. As discussed in section 3.2, the operator L is the negative of the second derivative operator with respect to arc length on each grain boundary segment. If η is twice continuously differentiable on each segment and satisfies the boundary conditions

$$\begin{array}{ll} 1. & \eta \text{ is continuous at } x_i \\ 2. & \mathcal{F}_i\eta = 0 \end{array} \qquad (i \text{ any junction label}), \tag{5.1}$$

then the restriction of $L\eta$ to the interior of Γ_j is given by

$$L\eta(x) = -\frac{\partial^2\eta}{\partial s^2} \qquad (x \in \Gamma_j^o). \tag{5.2}$$

Here $\mathcal{F}_i$ is a flux operator for junction i, defined by

$$\mathcal{F}_i\eta = (-1)^{k_i}\partial_s\eta(x_i) \qquad (x_i \text{ a gb-wall junction}), \tag{5.3}$$

$$\mathcal{F}_i\eta = \sum_{j=1}^{p_i}(-1)^{k_i^j}\partial_s\eta(x_i^j) \quad (x_i \text{ a gb junction of order } p_i), \tag{5.4}$$

where x_i^j is infinitesimally close to junction x_i on segment j and k_i^j is 0 or 1 depending on whether segment j is parameterized toward or away from x_i; see Figure 5.1. At junctions where a grain boundary meets an outer wall, only the second condition in (5.1) is imposed since the first condition is automatic.

5.2. Integration by parts on the network. Let $C(\Gamma)$ denote the space of continuous functions on Γ, and let $\widetilde{C}(\Gamma)$ denote the space of functions f continuous on the interiors of the Γ_j with well-defined limits $f(x_i^j)$ at the endpoints x_i of Γ_j but with possibly different limiting values at x_i when approached from different segments.

Differentiation is defined segment by segment, where we recall that each segment is given an arbitrary orientation along which the arc length parameter increases. We define

$$\widetilde{C}^r(\Gamma) = \{f : f^{(k)} \in \widetilde{C}(\Gamma),\ 0 \le k \le r\}. \tag{5.5}$$

For $f \in \widetilde{C}(\Gamma)$, we write

$$\left[f\right]_\Gamma = \sum_j \left[f(x^j_{i_1(j)}) - f(x^j_{i_0(j)})\right], \tag{5.6}$$

where $i_0(j)$ and $i_1(j)$ are the junction indices of the initial and final endpoints of segment j. We note that although both sides of (5.7) and (5.8) depend on the orientation chosen for each segment, the identities

$$\left[f'g\right]_\Gamma = \sum_i g(x_i)\mathcal{F}_i f \qquad \left(f \in \widetilde{C}^1(\Gamma)\ g \in C(\Gamma)\right) \tag{5.7}$$

and

$$\int_\Gamma f'g\,ds = \left[fg\right]_\Gamma - \int_\Gamma g'f\,ds \qquad \left(f, g \in \widetilde{C}^1(\Gamma)\right) \tag{5.8}$$

are valid for any particular choice. It follows that

$$(Lu, v) = (u, Lv) \qquad \left(u, v \in \widetilde{C}^2(\Gamma) \text{ and satisfy (5.1)}\right) \tag{5.9}$$

holds independently of the orientations chosen for each segment; i.e., the boundary value problem $Lu = \lambda u$ subject to the boundary conditions (5.1) is self-adjoint.

5.3. Construction of a Green's function. In this section we construct a Green's function $G_l(x, y)$ for the operator $L + l^2$, where l is any positive real number. Since L has a nontrivial kernel, there is no Green's function when $l = 0$. We begin by defining an auxiliary function

$$K_l(x, y) = \begin{cases} 0, & x, y \text{ on different segments,} \\ k_l(a_j, s_j(x), s_j(y)), & x, y \in \Gamma_j, \end{cases} \tag{5.10}$$

where $a_j = |\Gamma_j|$ is the length of Γ_j, $s_j(x) = |x - x_{i_0(j)}|$ is the value of the arc length parameter along Γ_j at x, and $k_l(a, x, y)$ is the Green's function for $-\partial_x^2 + l^2$ on the interval $(0, a)$ with Dirichlet boundary conditions; see Figure 5.2. For $(0 \le x \le y \le a)$, we have

$$k_l(a, x, y) = k_l(a, y, x) = \left(\cosh ly \frac{\sinh la}{l} - \cosh la \frac{\sinh ly}{l}\right) \frac{\sinh lx}{\sinh la}. \tag{5.11}$$

To get G_l from K_l, we have to fix the flux boundary conditions at each junction. Let n be the number of junctions, and define the linear operator $T_l : \mathbb{R}^n \to \mathbb{R}^n$ as follows. For $w \in \mathbb{R}^n$, let $u_{l,w}$ be the unique function in $C(\Gamma)$ which satisfies

$$u_{l,w}(x_i) = w_i, \quad \partial_s^2 u_{l,w} = l^2 u_{l,w}. \tag{5.12}$$

Explicitly, on segment Γ_j, we set

$$u_{l,w}(x) = w_{i_0(j)} \cosh ls_j(x) + \left[w_{i_1(j)} - w_{i_0(j)} \cosh la_j\right] \frac{\sinh ls_j(x)}{\sinh la_j}. \tag{5.13}$$

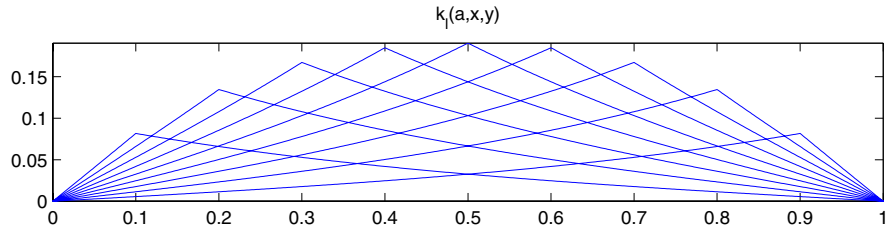

FIG. 5.2. *The function $k_l(a,x,y)$ satisfies $-\partial_x^2 k_l = l^2 k_l$ on $(0,y)$ and (y,a), is zero at $x=0$ and $x=a$, and has a unit (negative) jump in slope at $x=y$. In this plot, $a=1$, $l=2$, and $y=0.1,\dots,0.9$. Note that $\lim_{y\to 0}\frac{\partial}{\partial x}\big|_{x=0} k_l(a,x,y)=1$ with a similar result as $y\to 1$.*

Now we define the ith component of $T_l w$ to be the flux of $u_{l,w}$ into junction i:

$$(T_l w)_i = \mathcal{F}_i u_{l,w}. \tag{5.14}$$

Thus T_l converts values at junctions into fluxes at junctions of the solution to (5.12).

We next show that T_l is invertible. Suppose that $T_l w = 0$, i.e., that $\mathcal{F}_i u_{l,w} = 0$ at each junction. We wish to conclude that $u_{l,w} \equiv 0$, so we proceed by contradiction. Multiplying by (-1) if necessary, we assume the maximum value of $u_{l,w}$ is positive. The maximum cannot occur in the interior of a segment or at a gb-wall junction because the slope would be zero at such a maximum, while (5.12) would require that the second derivative be positive. It also cannot occur at a triple junction because the sum of the outward slopes is zero at such a junction: if any is positive it is not a maximum, and if each is zero we use (5.12) again. Thus we reach a contradiction and conclude that T_l is invertible.

To correct the flux boundary conditions of K_l to obtain G_l, we define $w_l(y) \in \mathbb{R}^n$ to give the values at the junctions of the solution to $\partial_x^2 u = l^2 u$ with the same junction fluxes as $K(\cdot,y)$:

$$w_l(y) = T_l^{-1}\left(\{\mathcal{F}_i K(\cdot,y)\}_{i=1}^n\right) \qquad (y \text{ not an endpoint}). \tag{5.15}$$

Note that $\mathcal{F}_i K(\cdot,y)$ is nonzero only when y is on a segment incident to junction i, and by (5.11), as y approaches junction i we have

$$\lim_{y\to x_i}\left(\{\mathcal{F}_k K(\cdot,y)\}_{k=1}^n\right) = -e_i \in \mathbb{R}^n. \tag{5.16}$$

We define $G_l(x,y)$ by

$$G_l(x,y) = \begin{cases} K(x,y) - u_{l,w_l(y)}(x), & y \text{ not an endpoint}, \\ u_{l,T_l^{-1}(e_i)}(x), & y = x_i. \end{cases} \tag{5.17}$$

By (5.16), $G_l(x,y)$ is continuous on $\Gamma\times\Gamma$, and by construction, for fixed y in the interior of some segment, $G_l(x,y)$ as a function of x satisfies the boundary conditions (5.1). It is readily verified using the corresponding property of $k_l(a,x,y)$ that the operator

$$\mathcal{G}_l f(x) = \int_\Gamma G_l(x,y) f(y)\, dy \tag{5.18}$$

is the inverse of $L + l^2$ in the sense that for all $f \in C(\Gamma)$ and all $u \in \widetilde{C}^2(\Gamma) \cap C(\Gamma)$ satisfying (5.1),

$$(L + l^2)\mathcal{G}_l f = f, \qquad \mathcal{G}_l(L + l^2)u = u. \tag{5.19}$$

$\mathcal{G}_l$ is self-adjoint since L is self-adjoint, and as a result, $G_l(x, y) = G_l(y, x)$ for all $x, y \in \Gamma$.

THEOREM 5.1. *There exists an orthonormal basis $\{\varphi_n\}_{n=1}^{\infty}$ for $L^2(\Gamma)$ and an increasing sequence of nonnegative numbers λ_n growing without bound such that*

$$\varphi_n \in \widetilde{C}^{\infty}(\Gamma) \cap C(\Gamma), \tag{5.20}$$

$$\mathcal{F}_i \varphi_n = 0 \qquad (i \text{ any junction label}), \tag{5.21}$$

$$L\varphi_n = \lambda_n^2 \varphi_n. \tag{5.22}$$

The domain of L satisfies

$$\{f \in \widetilde{C}^2(\Gamma) : f \text{ satisfies (5.1)}\} \subset \mathcal{D}(L) \subset \{f \in \widetilde{C}^1(\Gamma) : f \text{ satisfies (5.1)}\}. \tag{5.23}$$

Proof. In the standard way [7, 8], we can show that $\mathcal{G}_l$ is a self-adjoint, compact operator on $L^2(\Gamma)$; thus $\mathcal{G}_l$ has a complete orthonormal set $\{\varphi_n\}_{n=1}^{\infty}$ of eigenfunctions with eigenvalues converging to zero. It is also readily shown that for all $f \in L^1(\Gamma) \supset L^2(\Gamma)$,

$$\mathcal{G}_l f \in \{\eta \in \widetilde{C}^1(\Gamma) \,:\, \eta \text{ satisfies the boundary conditions (5.1)}\}; \tag{5.24}$$

hence the eigenfunctions are continuous and satisfy flux boundary conditions. Differentiating (5.18), it follows that if $f \in \widetilde{C}^r(\Gamma)$, then $\mathcal{G}_l f \in \widetilde{C}^{r+2}(\Gamma)$; thus the eigenfunctions belong to $\widetilde{C}^{\infty}(\Gamma)$ by a bootstrap argument. By (5.19), they are eigenfunctions of $L + l^2$ with reciprocal eigenvalues. Since $L + l^2$ is invertible for $l > 0$, we conclude that the eigenvalues of L form an unbounded sequence of nonnegative numbers $\{\lambda_n^2\}$. Finally, (5.23) holds when we *redefine* L to be $\mathcal{G}_l^{-1} - l^2$. Then $\mathcal{D}(L) = \operatorname{ran}(\mathcal{G}_l)$, so the first inclusion follows from (5.19) and the second from (5.24). ∎

5.4. The kernel of *L*. The segments Γ_j of the grain boundary network can be grouped together into connected components as sets in $\mathbb{R}^2$. We decompose the numbers $1, \dots, N$ into a collection $\mathcal{J}$ of disjoint sets such that each $J \in \mathcal{J}$ is the set of indices of the segments Γ_j that belong to component $\Gamma_J = \cup_{j \in J} \Gamma_j$. We number these subsets arbitrarily $\mathcal{J} = \{J_1, \dots, J_d\}$ and define the functions $e_k \in L^2(\Gamma)$ for $1 \le k \le d$ by

$$e_k(x) = \begin{cases} |\Gamma_{J_k}|^{-\frac{1}{2}}, & x \in \Gamma_{J_k}, \\ 0 & \text{otherwise.} \end{cases} \tag{5.25}$$

Here $|\Gamma_{J_k}| = \sum_{j \in J_k} |\Gamma_j|$ is the sum of the lengths of the segments making up component k. Note that each e_k is continuous at all junctions since all segments that meet at a junction belong to the same connected component.

PROPOSITION 5.2. *The functions $\{e_k\}_{k=1}^{d}$ form a basis for* $\ker(L)$.

Proof. Theorem 5.1 ensures that $\ker(L)$ is finite dimensional and is spanned by functions $\{\varphi_1, \dots, \varphi_{d'}\}$ satisfying (5.20)–(5.22) with $\lambda_n = 0$. Since each e_k also satisfies these conditions, we have $d' \ge d$, and it remains to show that any $\varphi \in \ker(L)$ is constant on each connected component. Suppose not. Then there is a segment Γ_{j*}

on which φ is not constant. Since $L\varphi = 0$, φ is linear on each segment. Starting with Γ_{j^*}, there is a path to an outer wall along which φ strictly increases. This is because φ satisfies (5.21), so if φ increases along a segment as we approach a triple junction, it must also increase along one of the other segments as we leave the junction. Since φ strictly increases along the path, no interior node can be revisited, and eventually the path reaches a wall with a positive slope, which contradicts (5.21). ∎

5.5. An isomorphism. In this section we show that $L^{\frac{1}{2}}$ becomes an isomorphism from $H^1(\Gamma)$ onto $L^2(\Gamma)$ if we modify it slightly to eliminate its kernel. It will be useful to define the operators

$$P = I - \sum_{n=1}^{d} (\cdot, \varphi_n)\varphi_n, \qquad A = L + \sum_{n=1}^{d} (\cdot, \varphi_n)\varphi_n. \tag{5.26}$$

Note that P is the orthogonal projection onto the subspace

$$\operatorname{ran}(L) = \ker(L)^{\perp} = \left\{ f \in L^2(\Gamma) \,:\, \int_{\Gamma_{J_k}} f\, ds = 0,\ 1 \le k \le d \right\} \tag{5.27}$$

and $L = AP = PA$. A and P are self-adjoint since the φ_n are orthogonal.

THEOREM 5.3. *For any absolutely continuous f such that $f' \in L^2(\Gamma)$, if we write $f = \sum a_n \varphi_n$, then*

$$\|f\|^2 = \sum_{n=1}^{\infty} |a_n|^2, \qquad \|f'\|^2 = \sum_{n=1}^{\infty} |a_n \lambda_n|^2. \tag{5.28}$$

There is a constant C such that

$$\|f\|_{L^2} \le \|A^{-\frac{1}{2}} f\|_{H^1} \le C \|f\|_{L^2} \qquad \big(f \in L^2(\Gamma)\big); \tag{5.29}$$

i.e., $A^{-\frac{1}{2}}$ is an isomorphism from $L^2(\Gamma)$ onto $H^1(\Gamma)$ and is therefore compact as an operator on $L^2(\Gamma)$. The domain of $L^{\frac{1}{2}}$ is $H^1(\Gamma)$, which requires continuity but imposes no constraints on the derivatives at junctions.

Proof. On each segment, we have

$$\varphi_n(x) = c_{n,j} \cos(\lambda_n s_j(x) - \theta_{n,j}) \qquad (x \in \Gamma_j). \tag{5.30}$$

We define

$$\psi_n = \lambda_n^{-1} \varphi_n' \qquad (n > d). \tag{5.31}$$

Note that ψ_n is *not* continuous on Γ but is zero at gb-wall junctions and satisfies appropriate jump conditions at triple junctions so that

$$\big[\psi_n g\big]_{\Gamma} = 0 \qquad (g \in C(\Gamma)). \tag{5.32}$$

We claim that $\{\psi_n\}_{n>d}$ is an orthonormal basis for the subset of functions $f \in L^2$ such that f is the derivative of an absolutely continuous function in $C(\Gamma)$. This subset will not be all of L^2 as soon as there are loops in the grain boundary network, since the integral around a loop must be zero for a continuous antiderivative to exist. By (5.8), we have the orthogonality condition

$$\int_{\Gamma} \psi_n \psi_m = \lambda_n^{-1} \left(\big[\varphi_n \psi_m\big]_{\Gamma} - \int_{\Gamma} \psi_m' \varphi_n \right) = \int_{\Gamma} \varphi_m \varphi_n = \delta_{mn}. \tag{5.33}$$

To prove completeness, suppose $W \in C(\Gamma)$ is absolutely continuous and $w = W'$ belongs to L^2. Suppose further that for all $n > d$, we have

$$\int_\Gamma w\psi_n = 0. \tag{5.34}$$

We must show that $w \equiv 0$. Integrating by parts, we obtain

$$\int_\Gamma w\psi_n = \big[W\psi_n\big]_\Gamma - \int_\Gamma \psi_n' W = \lambda_n \int_\Gamma W\varphi_n = 0 \qquad (n > d). \tag{5.35}$$

Since $\{\varphi_n\}_{n=1}^\infty$ is a basis, we conclude that W is a linear combination of $\varphi_1, \dots, \varphi_d$. Thus W is a constant on each connected component of Γ and $w = W' = 0$, as desired.

For any $f \in L^2$, we may expand $f = \sum_{n=1}^\infty a_n\varphi_n$ and apply the Parseval identity to conclude that $\|f\|^2 = \sum |a_n|^2$. If f is absolutely continuous and its derivative is in L^2, then we have $f' = \sum_{n>d} b_n\psi_n$ with

$$b_n = \int_\Gamma f'\psi_n = \big[f\psi_n\big]_\Gamma - \int_\Gamma f\psi_n' = \lambda_n \int_\Gamma f\varphi_n = \lambda_n a_n. \tag{5.36}$$

Since $\lambda_n = 0$ for $n \le d$, the Parseval identity gives the result $\|f'\|^2 = \sum_1^\infty |\lambda_n a_n|^2$. Therefore we have

$$\begin{aligned} \|f\|_{H^1}^2 &= \|f\|_{L^2}^2 + \|f'\|_{L^2}^2 = \sum_{n=1}^\infty (1+\lambda_n^2)|a_n|^2, \\ \|A^{\frac12} f\|_{L^2}^2 &= \sum_{n=1}^d |a_n|^2 + \sum_{n=d+1}^\infty \lambda_n^2 |a_n|^2. \end{aligned} \tag{5.37}$$

As a result, we obtain

$$\|A^{\frac12} f\|_{L^2} \le \|f\|_{H^1} \le C\|A^{\frac12} f\|_{L^2} \qquad \big(f \in H^1(\Gamma)\big), \tag{5.38}$$

with $C = \lambda_*^{-1}\sqrt{1+\lambda_*^2}$, where $\lambda_* = \lambda_{d+1}$ is the smallest nonzero eigenvalue of $L^{\frac12}$. ∎

DEFINITION 5.4. *The operator G is defined via*

$$G = A^{-1} - \sum_{n=1}^d (\cdot, \varphi_n)\varphi_n. \tag{5.39}$$

G is the pseudoinverse of L in the sense that they have the same kernel and eigenfunctions with reciprocal (or zero) eigenvalues. The properties of A imply that G is self-adjoint and compact on $L^2(\Gamma)$ and satisfies $G = PA^{-1} = A^{-1}P$ and $LG = P$.

6. Dynamics. In this section we show that if the grain boundary network is nondegenerate, then the equation

$$\eta_t = SL\eta, \qquad \eta(0) = \eta_0, \tag{6.1}$$

generates an analytic semigroup $\{E_t : t \ge 0\}$ of bounded linear operators on $H^1(\Gamma)$. See [31] for the degenerate case and the books [13, 32, 16, 1] for background information on semigroup theory. As mentioned in section 3.3, the solution $\eta(t)$ when the electromigration force is present is given by

$$\eta(t) = E_t(\eta_0 + \psi) - \psi. \tag{6.2}$$

The boundary conditions on η enforcing chemical potential continuity and flux balance at junctions hold as a consequence of the analyticity of E_t and the properties of the domain $\mathcal{D}(SL)$. The role of singularities in the stress field near corners and junctions is also discussed.

6.1. The semigroup generated by SL. In this section we show that there is a Riesz basis (a basis equivalent to an orthonormal basis [11]) for $H^1(\Gamma)$ consisting of eigenfunctions of SL. This allows us to exhibit the semigroup operator E_t explicitly, study its properties, and approximate it numerically [30, 26]. Throughout this section, we assume the grain boundary network is nondegenerate so that B is injective and $SB = I$ on $L^2(\Gamma)$.

LEMMA 6.1. *Let us denote* $\ker(L) = \operatorname{span}\{e_k\}_{k=1}^d$ *by* $\{e\}$. *Then*

$$\ker(SL) = \{e\}, \qquad \operatorname{ran}(SL) = \{Be\}^\perp. \tag{6.3}$$

Proof. SL is densely defined in $L^2(\Gamma)$ since $\mathcal{D}(S)$ is dense, A^{-1} is bounded with dense range, and $\mathcal{D}(SL) = A^{-1}\mathcal{D}(S)$. Clearly $\{e\} \subset \ker(SL)$. Since S is injective on its domain, if $Lx \in \mathcal{D}(S)$ is nonzero, so is SLx. Thus $\ker(SL) = \{e\}$ as claimed. Suppose $y = SLx$. Then $By = Lx$ belongs to $\operatorname{ran}(L) = \{e\}^\perp$, so $(y, Be) = 0$ for all $e \in \ker(L)$, as claimed. ∎

LEMMA 6.2. *The (nonorthogonal) projection on* $L^2(\Gamma)$ *given by*

$$Q \text{ projects along } \{e\} \text{ onto } \{Be\}^\perp \tag{6.4}$$

is well defined.

Proof. Since B is injective, $\{e\}$ and $\{Be\}$ have the same dimension. We must show that $\{e\} \cap \{Be\}^\perp = \{0\}$. Suppose $x \in \{e\} \cap \{Be\}^\perp$. Then $(x, Bx) = 0$, which implies $x = 0$ since B is self-adjoint and negative definite. ∎

Remark 6.3. Q may be written explicitly as $I - (\cdot, w_k)e_k$ (summation implied), where $w_k = (Be_j)\alpha_{jk}$ and $(e_i, Be_j)\alpha_{jk} = \delta_{ik}$. Since the L^2 inner product $(\cdot, w_k)$ is a bounded linear functional on $H^1(\Gamma)$ and $e_k \in H^1(\Gamma)$, Q is also a well-defined projection on $H^1(\Gamma)$. By contrast, the L^2 adjoint $Q^* = I - (\cdot, e_k)w_k$ is generally not defined on $H^1(\Gamma)$ due to the possibility of singularities in the arc length derivative of w_k near junctions.

LEMMA 6.4. *The following diagram is commutative in the sense that for each block* $X \underset{g}{\overset{f}{\rightleftarrows}} Y$ *we have* $f \circ g = id_Y$ *and* $g \circ f = id_{\mathcal{D}(f)}$:

$$\{Be\}^\perp \underset{Q}{\overset{P}{\rightleftarrows}} \{e\}^\perp \underset{G}{\overset{L}{\rightleftarrows}} \{e\}^\perp \underset{B}{\overset{S}{\rightleftarrows}} \{Be\}^\perp . \tag{6.5}$$

Proof. P and Q both project along $\{e\}$, so $PQ = P$ and $QP = Q$. Since $\operatorname{ran}(P) = \{e\}^\perp$ and $\operatorname{ran}(Q) = \{Be\}^\perp$, the block involving P and Q is commutative. Since LG is the identity on $\{e\}^\perp$ and GL is the identity on $\mathcal{D}(L) \cap \{e\}^\perp = \operatorname{ran}(G)$, the block involving L and G is commutative. If $(x, Be) = 0$, then $(Bx, e) = 0$, so B maps $\{Be\}^\perp$ to $\{e\}^\perp$. Since SB is the identity on $L^2(\Gamma)$ and BS is the identity on $\mathcal{D}(S) = \operatorname{ran}(B)$, the block involving S and B is commutative. ∎

THEOREM 6.5. *There is a Riesz basis* $\{\phi_k\}$ *for* $H^1(\Gamma)$ *and a nonincreasing, unbounded sequence of numbers* $\lambda_k \le 0$ *such that* $SL\phi_k = \lambda_k\phi_k$.

Proof. The operator $K = G^{\frac{1}{2}}Q^*BQG^{\frac{1}{2}}$ is compact and self-adjoint, so there is an orthonormal basis $\{\varphi_k\}$ for $L^2(\Gamma)$ such that $K\varphi_k = \mu_k\varphi_k$, ($\mu_k \in \mathbb{R}$, $\mu_k \to 0$). Note

that $\mu_k = (\varphi_k, K\varphi_k) = (QG^{\frac{1}{2}}\varphi_k, BQG^{\frac{1}{2}}\varphi_k) \le 0$, with equality iff $QG^{\frac{1}{2}}\varphi_k = 0$. Note that $\ker(QG^{\frac{1}{2}}) = \ker(G^{\frac{1}{2}}) = \{e\}$ since $\ker(Q) = \{e\}$ and $\operatorname{ran}(G^{\frac{1}{2}}) \subset \{e\}^\perp$. We may therefore assume $\mu_1, \dots, \mu_d = 0$, and the remaining μ_k form an increasing sequence of negative numbers converging to zero. Note that

$$QGQ^*B(QG^{\frac{1}{2}}\varphi_k) = \mu_k(QG^{\frac{1}{2}}\varphi_k). \tag{6.6}$$

From the above remarks, we know $QG^{\frac{1}{2}}\varphi_k$ is nonzero for $k > d$. We define

$$\phi_k = \left\{ \begin{array}{ll} \varphi_k, & k = 1, \dots, d \\ QG^{\frac{1}{2}}\varphi_k, & k > d \end{array} \right\}, \quad \lambda_k = \left\{ \begin{array}{ll} 0, & k = 1, \dots, d \\ \mu_k^{-1}, & k > d \end{array} \right\}. \tag{6.7}$$

From the definition of Q, it follows that $Q^*B = BQ$, so $QGBQ\phi_k = \mu_k\phi_k$. If $k \le d$, then $SL\phi_k = 0$ since $\phi_k \in \{e\}$. Otherwise, $Q\phi_k = \phi_k$ and Lemma 6.4 gives $SL\phi_k = SL(\mu_k^{-1}QGB\phi_k) = \lambda_k\phi_k$. It is readily verified that for $k \ge 1$,

$$\phi_k = \left[(I - P) + QG^{\frac{1}{2}}\right]\varphi_k, \qquad \varphi_k = \left[(I - Q) + L^{\frac{1}{2}}\right]\phi_k. \tag{6.8}$$

Since $[I - P + QG^{\frac{1}{2}}]$ is bounded from $L^2(\Gamma)$ to $H^1(\Gamma)$ and its inverse $[I - Q + L^{\frac{1}{2}}]$ is bounded in the other direction, they are isomorphisms. Thus the ϕ_k form a Riesz basis for $H^1(\Gamma)$ as claimed. ∎

THEOREM 6.6. *The initial value problem $\eta_t = SL\eta$, $\eta(0) = \eta_0$ generates an analytic semigroup $\{E_t : t \ge 0\}$ of bounded linear operators on $H^1(\Gamma)$.*

Proof. Since the ϕ_k form a Riesz basis, the mapping from $H^1(\Gamma)$ to l^2 giving the coefficients of the expansion $\eta_0 = \sum_k a_k\phi_k$ is an isomorphism, and there is a constant C independent of η_0 such that $C^{-2}\|\eta_0\|_{H^1}^2 \le \sum_{k=1}^\infty |a_k|^2 \le C^2\|\eta_0\|_{H^1}^2$. These coefficients may be determined via

$$a_k = ([I - Q + L^{\frac{1}{2}}]\eta_0, \varphi_k) = (\eta_0, \phi_k^*), \qquad \phi_k^* = [I - Q^* + L^{\frac{1}{2}}]\varphi_k, \tag{6.9}$$

where $(\cdot, \cdot)$ is the $L^2(\Gamma)$ inner product. For $\eta_0 \in H^1(\Gamma)$ we define

$$E_t\eta_0 = \textstyle\sum_k a_k e^{\lambda_k t}\phi_k, \qquad a_k = (\eta_0, \phi_k^*). \tag{6.10}$$

E_t is bounded for any $t \ge 0$ since $\lambda_k \le 0$ for all k, and hence $\|E_t\eta_0\|_{H^1} \le C^2\|\eta_0\|_{H^1}$. E_0 is clearly the identity on $H^1(\Gamma)$, and $E_{t+s} = E_tE_s$ since $(\phi_j, \phi_k^*) = \delta_{jk}$. For fixed η_0, the mapping $t \mapsto E_t\eta_0$ is continuous for $t \ge 0$ since

$$\|E_t\eta_0 - E_s\eta_0\|_{H^1} \le C\left(\sum_{k=1}^N |a_k(e^{\lambda_k t} - e^{\lambda_k s})|^2 + \sum_{k=N+1}^\infty |a_k|^2\right)^{\frac{1}{2}} \tag{6.11}$$

may be made arbitrarily small by choosing N large enough to make the second term small and then s close enough to t to make the first term small. Note that for any fixed $t > 0$ and $\eta_0 \in H^1(\Gamma)$ we have

$$\left\|\frac{E_{t+h}\eta_0 - E_t\eta_0}{h} - SLE_t\eta_0\right\|_{H^1} \le C\left(\sup_{k\ge1}\left|t^{-1}f_1(\lambda_k t)f_2(\lambda_k h)\right|\right)\left(\sum_{k=1}^\infty |a_k|^2\right)^{\frac{1}{2}}, \tag{6.12}$$

where $f_1(z) = ze^z$ and $f_2(z) = \frac{1}{z}(e^z - 1) - 1$. The supremum may be made arbitrarily small by taking h sufficiently close to zero since f_1 and f_2 are bounded on

the negative real axis, $\lim_{z\to-\infty} f_1(z) = 0$, and $\lim_{z\to 0} f_2(z) = 0$. Thus we see that SL is the generator of $\{E_t : t \geq 0\}$. To show that this semigroup is analytic, we need only check that $\limsup_{t\downarrow 0} t\|SLE_t\| < \infty$, which follows from $t\|SLE_t\eta_0\|_{H^1} \leq C\left(\sup_k |f_1(\lambda_k t)|\right)\left(\sum_1^\infty |a_k|^2\right)^{1/2} \leq C^2 e^{-1}\|\eta_0\|_{H^1}$. ∎

Remark 6.7. Equation (6.10) leads to a useful numerical method in which ϕ_k, ϕ_k^*, and λ_k are computed by approximating $QGBQ$ (which has the same eigenfunctions as SL with reciprocal or zero eigenvalues) using a singularity capturing least squares finite element method; see [30, 26].

Remark 6.8. Since E_t is an operator on $H^1(\Gamma)$ and the formula for the evolution of normal stress is given by

$$\eta(t) = E_t(\eta_0 + \psi) - \psi, \tag{6.13}$$

we should verify that ψ belongs to $H^1(\Gamma)$. Since ψ is the solution to the Laplace equation on a domain with corners, it is smooth in the interior of Ω with singularities of the form

$$r^\lambda \phi(\theta) \qquad (\lambda = \pi/\omega \geq 1/2) \tag{6.14}$$

near reentrant corners of opening angle $\omega \leq 2\pi$ [12, 19]. As a result, the restriction of ψ to Γ is continuous on Γ, differentiable in the interior of each Γ_j, and its derivative with respect to arc length cannot diverge at the endpoints faster than $s^{(\lambda_{\min}-1)}$. (It will diverge at all only if the grain boundary terminates at a reentrant corner of the domain.) If we assume that Ω has no cracks with $\omega = 2\pi$ or, if it has cracks, that the crack tips do not lie on grain boundaries, then $\lambda_{\min} > \frac{1}{2}$ and $\psi \in H^1(\Gamma)$ as claimed.

6.2. The steady state stress distribution. Since $\lambda_1 = \cdots = \lambda_d = 0$, E_t leaves $\{e\} = \ker(SL)$ invariant. Since $\lambda_k \leq \lambda_{d+1} < 0$ for $k > d$, E_t takes any vector in $\{Be\}^\perp = \mathrm{ran}(SL)$ to zero as $t \to \infty$. More precisely, one may show [31] that $\lim_{t\to\infty} E_t = I - Q$ in norm. Thus

$$\eta_{\text{steady}} = \lim_{t\to\infty} \eta(t) = (I - Q)(\eta_0 + \psi) - \psi. \tag{6.15}$$

As a result, in the nondegenerate case there are constants c_j such that

$$\eta_{\text{steady}} = -\psi + c_j e_j \qquad \text{(summation implied)}. \tag{6.16}$$

We also observe that $(\eta_{\text{steady}} - \eta_0) = -Q(\eta_0 + \psi) \in \{Be\}^\perp$, so

$$(\eta_{\text{steady}} - \eta_0, Be_k) = 0 \qquad (1 \leq k \leq d). \tag{6.17}$$

Since B is self-adjoint, this implies $(g_{\text{steady}} - g_0, e_k) = 0$, which is a statement of mass conservation on each connected component of Γ. Using (6.16) and (6.17), we have

$$c_j(e_j, Be_k) = (\eta_0 + \psi, Be_k) \qquad (1 \leq k \leq d), \tag{6.18}$$

which determines the c_j uniquely due to the fact that the $d\times d$ matrix with components (e_j, Be_k) is invertible. Note that the steady state flux $\partial_s(\eta_{\text{steady}}+\psi)$ is zero; this ceases to be true in the degenerate case [31], where (6.16) has additional nonconstant terms.

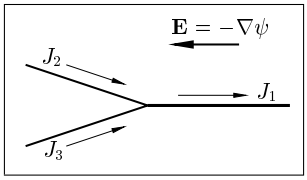

FIG. 6.1. *The electric field can lead to a flux imbalance at a triple (or wall) junction which must be immediately compensated by stress gradients to satisfy mass conservation. As a result, ψ generally will not lie in $\mathcal{D}(L)$ although $\eta(t) + \psi \in \mathcal{D}(L)$ when $t > 0$.*

6.3. Boundary conditions. ψ does not necessarily satisfy zero flux boundary conditions at junctions, and therefore, although $\psi \in \mathcal{D}(L^{1/2})$, it is not necessarily in $\mathcal{D}(L)$; see Figure 6.1. On the other hand, because E_t is analytic, we have range$(E_t) \subset \mathcal{D}(SL)$ for all $t > 0$. Therefore $\eta(t)$ in (6.13) has the property that

$$\eta(t) + \psi \in \mathcal{D}(L) \qquad (t > 0). \tag{6.19}$$

This implies chemical potential continuity and flux balance at all junctions for $t > 0$ (conditions 4b, 5b, and 5c in Figure 2.3). The grain growth function g may be obtained from η via $g(t) = B\eta(t)$, which automatically satisfies the compatibility conditions 4a and 5a of Figure 2.3 by virtue of the definition of B in (4.6). We have therefore proved that the grain boundary diffusion problem is well posed.

6.4. Stress singularities at junctions. It is well known that solutions to elliptic systems (such as the Lamé equations) on domains with corners and interface junctions exhibit singularities at these junctions. In the current case, as the normal stress η evolves on the grain boundary network, the stress and displacement fields in the bulk grains evolve as the solution to the grain boundary normal stress problem with η specified on Γ; see Definition 4.1. The general theory [30, 19, 24] states that the singular part of the solution may be written as a sum of power solutions (each component of the form $r^\lambda \phi(\theta)$ in local polar coordinates) to the *homogeneous* boundary value problem. As a result, the singular part of the solution near a given junction satisfies boundary conditions (4.1)–(4.4) with $\eta \equiv 0$ along the grain boundaries entering the junction. Although a different linear combination of stress components will generally diverge as the junction is approached along Γ, $\mathbf{n} \cdot \sigma\mathbf{n}$ will remain finite and well behaved, and all boundary conditions in Figure 2.3 describe quantities that remain finite despite the singularities. The corresponding displacement jump g will also remain finite, although it will generally exhibit infinite slopes and discontinuities (compatible with the boundary conditions) at junctions.

We have therefore demonstrated a mechanism through which stress components directly involved in the mass transport process remain bounded and well behaved while other "hidden" stress components grow very large and develop singularities; these components may be responsible for void nucleation and stress-induced damage but are omitted from commonly used scalar stress-generation models. In [30, 26], the first several terms in the asymptotic expansion for $\mathbf{u}$ and σ are computed a priori and added to the finite element basis to improve accuracy without mesh refinement. These singular functions often are very complicated, with singularity exponents clustered together in the complex plane.

Appendix. Infinite interconnect line.

In this section, we work out an exact solution to the stress-driven grain boundary diffusion problem $g_t = -\eta_{xx}$ for an infinite interconnect line with a single grain

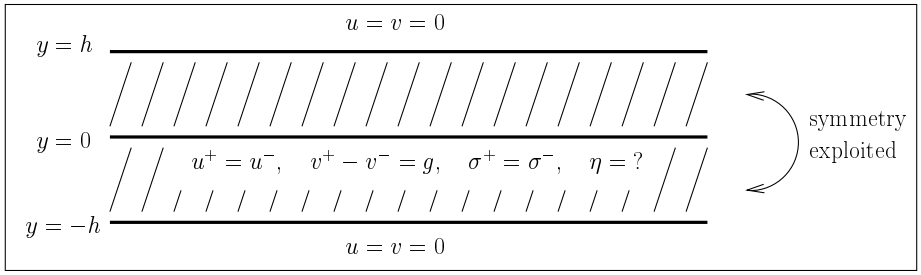

FIG. A.1. *The geometry and boundary conditions for the infinite strip.*

boundary running through the center. This provides useful insight about the nature of the diffusion process without the complication of boundary conditions at junctions or singularities in the stress field. The approach is to solve the elastic equations for a sinusoidal grain growth g and then use separation of variables and the Fourier transform to determine the evolution for an arbitrary initial condition.

A.1. Elastic equations for sinusoidal grain growth. Suppose the grain boundary coincides with the x-axis, and let h denote the width of each grain, as shown in Figure A.1. If we let $u = u_1$, $v = u_2$ and define κ, α, β, γ, and τ by

$$\kappa = \frac{\lambda + 3\mu}{\lambda + \mu}, \qquad \sigma = \mu \begin{pmatrix} \alpha - \gamma & \tau \\ \tau & \alpha + \gamma \end{pmatrix}, \qquad \beta = \frac{2}{\kappa + 1}(v_x - u_y), \tag{A.1}$$

then complex variable methods in plane elasticity [22, 30] can be used to guarantee the existence of holomorphic ϕ and ψ (known as Muskhelishvili functions) such that

$$\begin{aligned} \alpha + i\beta &= 2\phi', \\ \gamma + i\tau &= \bar{z}\phi'' + \psi', \\ u + iv &= \frac{1}{2}\left(\kappa\phi - z\bar{\phi}' - \bar{\psi}\right). \end{aligned} \tag{A.2}$$

By symmetry, for any displacement jump $g(x)$ the variables in the top grain will be related to the variables in the bottom grain via

$$u^+(x,y) = u^-(x,-y), \qquad v^+(x,y) = -v^-(x,-y), \tag{A.3}$$

$$\alpha^+(x,y) = \alpha^-(x,-y), \qquad \beta^+(x,y) = -\beta^-(x,-y), \tag{A.4}$$

$$\gamma^+(x,y) = \gamma^-(x,-y), \qquad \tau^+(x,y) = -\tau^-(x,-y). \tag{A.5}$$

Thus it is sufficient to restrict attention to the top grain. At $y = h$, we impose Dirichlet boundary conditions $u = v = 0$. Along the grain boundary, the four conditions $u^+ = u^-$, $v^+ - v^- = g$, $\alpha^+ + \gamma^+ = \alpha^- + \gamma^-$, $\tau^+ = \tau^-$ reduce to

$$\tau = 0, \qquad v = \frac{g}{2} \qquad \text{(boundary conditions along grain boundary)}. \tag{A.6}$$

We observe that in the limit as $h \to \infty$, these boundary conditions coincide with the problem of a rigid stamp without friction on a half-space and can be solved using singular integrals [23]. We omit details since the result for finite h covers this case in the limit.

For finite h, the singular integral approach does not work (at least not easily), so instead we take g of the form

$$g(x) = c_1 \cos \omega x + c_2 \sin \omega x \tag{A.7}$$

and make an ansatz for the form of the Muskhelishvili functions:

$$\phi = (a_1 + ia_2)\cos \omega z + (a_3 + ia_4)\sin \omega z, \tag{A.8}$$

$$\psi = (a_5 + ia_6)\cos \omega z + (a_7 + ia_8)\sin \omega z + (a_9 + ia_{10})z\cos \omega z + (a_{11} + ia_{12})z \sin \omega z. \tag{A.9}$$

We wish to determine if there are real coefficients a_i for which the boundary conditions are satisfied. We begin by constructing the 4×12 real matrix $A_0(\omega, \kappa, h, x)$ whose ith column contains the boundary conditions $u(y = h)$, $v(y = h)$, $v(y = 0)$, $\tau(y = 0)$ for the ϕ and ψ corresponding to a_i. For example, the second column corresponds to $\phi = i \cos \omega z$, $\psi = 0$:

$$\operatorname{col}_2(A_0) = \frac{1}{2}\begin{pmatrix} \omega h \sin \omega x \cosh \omega h - \omega x \cos \omega x \sinh \omega h + \kappa \sin \omega x \sinh \omega h \\ -\omega h \cos \omega x \sinh \omega h - \omega x \sin \omega x \cosh \omega h + \kappa \cos \omega x \cosh \omega h \\ -\omega x \sin \omega x + \kappa \cos \omega x \\ -2\omega^2 x \cos \omega x \end{pmatrix}. \tag{A.10}$$

Next we define the 16×12 real matrix $A(\omega, \kappa, h)$ by expanding each row of A_0 into four rows containing the coefficients of $\cos(\omega x)$, $\sin(\omega x)$, $x\cos(\omega x)$, $x\sin(\omega x)$. To satisfy the boundary conditions (A.6), we need to find $a \in R^{12}$ such that $Aa = b$, where b contains the desired coefficients of the terms $\cos(\omega x)$, $\sin(\omega x)$, $x\cos(\omega x)$, $x\sin(\omega x)$ in the boundary conditions. Explicitly, b and the second column of A are given by

$$b = \frac{1}{2}\begin{pmatrix} 0 \\ 0 \\ 0 \\ 0 \\ 0 \\ 0 \\ 0 \\ 0 \\ c_1 \\ c_2 \\ 0 \\ 0 \\ 0 \\ 0 \\ 0 \\ 0 \end{pmatrix}, \qquad \operatorname{col}_2(A) = \frac{1}{2}\begin{pmatrix} 0 \\ \omega h \cosh \omega h + \kappa \sinh \omega h \\ -\omega \sinh \omega h \\ 0 \\ -\omega h \sinh \omega h + \kappa \cosh \omega h \\ 0 \\ 0 \\ -\omega \cosh \omega h \\ \kappa \\ 0 \\ 0 \\ -\omega \\ 0 \\ 0 \\ -2\omega^2 \\ 0 \end{pmatrix}. \tag{A.11}$$

We verify that a solution exists by computing the nullspace of A^T symbolically and checking that $b \in (\ker A^T)^\perp = \text{image } A$. We then select 12 linearly independent rows of A (and the corresponding rows of b) and solve $Aa = b$ symbolically. The resulting a determines ϕ and ψ, which we use to compute $\eta = \sigma_{22} = \alpha + \gamma$ along the grain boundary. This has to be done only once since the parameters such as κ and h appear

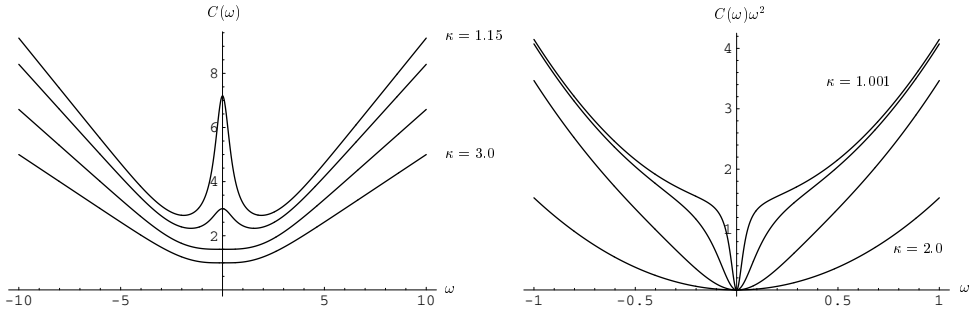

FIG. A.2. *Left: plot of $C(\omega)$ for $h = 1$ and $\kappa = 1.15, 1.4, 2.0, 3.0$. Right: plot of the dissipation rate $C(\omega)\omega^2$ for $h = 1$ and $\kappa = 1.001, 1.01, 1.1, 2.0$. Note that $C(\omega)$ diverges in the incompressible ($\kappa \to 1$), long wavelength ($\omega \to 0$) limit and that although $C(\omega)$ is not monotonic for $\kappa < 2$, $C(\omega)\omega^2$ is monotonic for $\omega \geq 0$. The envelope of the graphs of $C(\omega)\omega^2$ is $\frac{3}{2} + \frac{27}{10}\omega^2$ near the origin as $\kappa \to 1$.*

symbolically. All of this, including the construction of A_0 and A via (A.2), (A.8), and (A.9), can be done without difficulty using Mathematica or Maple.

The result of this computation is that along the grain boundary, η is a constant multiple of g for any c_1, c_2, ω:

$$\eta(x) = -C(\omega)g(x), \qquad C(\omega) = \frac{\omega[1 + \kappa^2 + 4h^2\omega^2 + 2\kappa\cosh 2h\omega]}{(1+\kappa)[\kappa \sinh 2h\omega - 2h\omega]}. \tag{A.12}$$

A plot of $C(\omega)$ for a few values of κ is given in Figure A.2. For large and small ω, we see that $C(\omega)$ has the asymptotic form

$$C(\omega) = \frac{2\omega}{1+\kappa} \qquad (|h\omega| \gg 1), \tag{A.13}$$

$$C(\omega) = \frac{1}{h}\left\{\frac{\kappa+1}{2(\kappa-1)} - \frac{(\kappa-2)(\kappa-3)}{3(\kappa-1)^2}(h\omega)^2 + \cdots\right\} \qquad (|h\omega| \ll 1). \tag{A.14}$$

A.2. Evolution for an arbitrary initial condition. The fact that $\eta(x) = -C(\omega)g(x)$ when g varies harmonically allows us to use the Fourier transform to solve the grain boundary diffusion problem for an arbitrary initial condition $g(x, t = 0)$. Note that the solution to $g_t = -\eta_{xx}$ with $g(x, t = 0) = \cos\omega x$ is given by

$$g(x,t) = e^{-C(\omega)\omega^2 t}\cos\omega x. \tag{A.15}$$

This gives the time evolution of each Fourier mode. If we write g at $t = 0$ as

$$g(x,0) = \int_{-\infty}^{\infty} e^{i\omega x}\hat{g}(\omega,0)\,d\omega, \tag{A.16}$$

then at any later time g will be

$$g(x,t) = \int_{-\infty}^{\infty} e^{i\omega x}\hat{g}(\omega,t)\,d\omega = \int_{-\infty}^{\infty} e^{i\omega x}e^{-C(\omega)\omega^2 t}\hat{g}(\omega,0)\,d\omega. \tag{A.17}$$

It is instructive to compare the dissipation rate $C(\omega)\omega^2$ to that for the heat equation and the linearized surface diffusion equation:

Dissipation Rate	Equation
$b\omega^2$	$u_t = bu_{xx} \quad (b > 0)$
$C(\omega)\omega^2$	$g_t = -\eta_{xx}$
$b\omega^4$	$u_t = -bu_{xxxx} \quad (b > 0)$

From Figure A.2 and (A.12)–(A.14), we see that low-frequency modes decay like the heat equation with $b = (\kappa+1)[2h(\kappa-1)]^{-1}$, whereas high-frequency modes decay as $\exp(-b|\omega|^3)$ with $b = 2(1+\kappa)^{-1}$, which is halfway between the heat equation and the linearized surface diffusion equation.

REFERENCES

[1] V. Barbu, *Nonlinear Semigroups and Differential Equations in Banach Spaces*, Noordhoff, Leyden, The Netherlands, 1976.

[2] I. A. Blech, *Electromigration in thin aluminum films on titanium nitride*, J. Appl. Phys., 47 (1976), pp. 1203–1208.

[3] I. A. Blech and C. Herring, *Stress generation by electromigration*, Appl. Phys. Lett., 29 (1976), pp. 131–133.

[4] A. F. Bower and D. Craft, *Analysis of failure mechanisms in the interconnect lines of microelectronic circuits*, Fatigue Fract. Engrg. Mater. Struct., 21 (1998), pp. 611–630.

[5] P. G. Ciarlet, *Mathematical Elasticity*, Vol. 1, North–Holland, Amsterdam, 1993.

[6] A. C. F. Cocks and S. P. A. Gill, *A variational approach to two dimensional grain growth I. Theory*, Acta Mater., 44 (1996), pp. 4765–4775.

[7] E. A. Coddington and N. Levinson, *Theory of Ordinary Differential Equations*, Krieger, Malabar, FL, 1984.

[8] R. Courant and D. Hilbert, *Methods of Mathematical Physics*, Vol. I, Wiley Interscience, New York, 1989.

[9] V. B. Fiks, *Mechanism of ion mobility in metals*, Soviet Physics—Solid State, 1 (1959), pp. 14–28.

[10] D. Fridline, *Finite Element Modeling of Electromigration and Stress Voiding in Microelectronic Interconnects*, Ph.D. thesis, Brown University, Providence, RI, 2001.

[11] I. C. Gohberg and M. G. Krein, *Introduction to the Theory of Linear Nonselfadjoint Operators*, Transl. Math. Monogr. 18, AMS, Providence, RI, 1969.

[12] P. Grisvard, *Singularities in Boundary Value Problems*, Res. Notes Appl. Math. 22, Masson, Paris, 1992.

[13] E. Hille and R. S. Phillips, *Functional Analysis and Semi-groups*, AMS, Providence, RI, 1957.

[14] P. S. Ho and T. Kwok, *Electromigration in metals*, Rep. Prog. Phys., 52 (1989), pp. 301–348.

[15] H. Huntington and A. Grone, *Current-induced marker motion in gold wires*, J. Phys. Chemistry Solids, 20 (1961), pp. 76–87.

[16] T. Kato, *Perturbation Theory for Linear Operators*, Springer-Verlag, Berlin, 1980.

[17] R. Kirchheim, *Stress and electromigration in Al-lines of integrated circuits*, Acta Metal. Mater., 40 (1992), pp. 309–323.

[18] M. A. Korhonen, P. Borgesen, K. N. Tu, and C.-Y. Li, *Stress evolution due to electromigration in confined metal lines*, J. Appl. Phys., 73 (1993), pp. 3790–3799.

[19] V. A. Kozlov, V. G. Maz'ya, and J. Rossmann, *Elliptic Boundary Value Problems in Domains with Point Singularities*, AMS, Providence, RI, 1997.

[20] L. D. Landau and E. M. Lifshitz, *Theory of Elasticity*, 3rd ed., Butterworth–Heinemann, Oxford, UK, 1986.

[21] W. W. Mullins, *Mass transport at interfaces in single component systems*, Metal. Mater. Trans. A, 26 (1995), pp. 1917–1929.

[22] N. I. Muskhelishvili, *Some Basic Problems of the Mathematical Theory of Elasticity*, 2nd English ed., P. Noordhoff, Groningen, The Netherlands, 1963.

[23] N. I. Muskhelishvili, *Singular Integral Equations*, 2nd ed., Dover, New York, 1992.

[24] B. A. Plamenevskij, *Elliptic boundary value problems in domains with piecewise smooth boundary*, in Partial Differential Equations 9, Encyclopaedia Math. Sci. 79, M. S. Agranovich, Y. V. Egorov, and M. A. Shubin, eds., Springer-Verlag, Berlin, 1997.

[25] M. E. Sarychev, Y. V. Zhitnikov, L. Borucki, C. L. Liu, and T. M. Makhviladze, *General model for mechanical stress evolution during electromigration*, J. Appl. Phys., 86 (1999), pp. 3068–3075.

[26] J. A. Sethian and J. Wilkening, *A numerical model of stress driven grain boundary diffusion*, J. Comput. Phys., 193 (2003), pp. 275–305.
[27] R. S. Sorbello, *Theory of electromigration*, in Solid State Physics, Vol. 51, H. Ehrenreich and F. Spaepen, eds., Academic Press, New York, 1997, pp. 159–231.
[28] B. G. Streetman and S. Banerjee, *Solid State Electronic Devices*, Prentice–Hall, Englewood Cliffs, NJ, 2000.
[29] K.-N. Tu, J. W. Mayer, and L. C. Feldman, *Electronic Thin Film Science for Electrical Engineers and Materials Scientists*, Macmillan, New York, 1992.
[30] J. Wilkening, *Mathematical Analysis and Numerical Simulation of Electromigration*, Ph.D. thesis, University of California, Berkeley, 2002.
[31] J. Wilkening, L. Borucki, and J. A. Sethian, *Analysis of stress-driven grain boundary diffusion. Part* II*: Degeneracy*, SIAM J. Appl. Math., 64 (2004), pp. 1864–1886.
[32] K. Yosida, *Functional Analysis*, Springer-Verlag, Heidelberg, 1980.
[33] P. V. Zant, *Microchip Fabrication: A Practical Guide to Semiconductor Processing*, McGraw–Hill, New York, 2000.